Collision-Induced Dissociation of Cesium Iodide Cluster Ions. Scattering Angular Distribution and Excitation Mechanism

Young Jin Lee[†] and Myung Soo Kim*

Department of Chemistry and Center for Molecular Catalysis, Seoul National University, Seoul 151-742, Korea

Received: December 16, 1996; In Final Form: June 13, 1997[⊗]

Collision-induced dissociation (CID) of cesium iodide cluster ions was investigated at kiloelectronvolt laboratory translational energy using "light" (H_2, D_2, and He) and "heavy" (Ne, Ar, and Xe) collision gases. Substantial translational energy losses were observed with light targets, as was the case with polypeptide ions with similar masses reported previously. In the present case, the large energy losses were mainly due to the elastic energy transfer to the targets. From the translational energy profiles of CID product ions, energetic and dynamic data, and, in particular, the scattering angular distribution, were obtained. The angular distributions obtained with H_2, D_2, and He were virtually identical at the same center-of-mass translational energy while the one with Ne was different. This suggested that the energy transfer mechanism with light targets might be different from that with heavy ones. Theoretical calculations with a binary collision model could explain the angular distributions with Ne, suggesting that vibrational excitation via momentum transfer is a possible candidate mechanism. Even though the angular distributions could not be determined for CID with Xe or Ar collision gases, the same conclusion can be made based on the basis of the magnitudes of the translational energy loss. On the other hand, those with light targets could not be explained with the above model indicating the dominance of vibronic excitation.

Introduction

Reactions of large polyatomic molecules, either natural or synthetic, have become an important research subject in chemistry. In particular, collision-induced dissociation (CID) of large polyatomic ions at superthermal energy (10−10 000 eV)[1−4] is attracting much attention because the phenomenon is useful in mass spectrometry for structural characterization of large molecules.[5−8]

The CID process is generally thought to occur in two separate steps,[9−11] the collisional excitation and dissociation steps, even though some exceptions are known.[12]

$$m_1^+ \xrightarrow{N} m_1^{+*} \quad (1)$$

$$m_1^{+*} \rightarrow m_2^+ + m_3 \quad (2)$$

Here, m_1^+ and N are the parent ion (projectile) and the collision gas (target) and m_2^+ and m_3 are the product ion and neutral, respectively. m_1^{+*} represents the parent ion excited by collision. Each of these steps has been the focus of tremendous research interest. Even though statistical theories such as the Rice−Ramsperger−Kassel−Marcus (RRKM) theory are generally accepted to account for the dissociation of simple polyatomic ions,[13,14] the dissociation mechanism of larger systems (for example, *m*/*z* 1000 or larger, number of atoms 100 or larger) is still an outstanding problem.[15−17] The fundamental understanding on the first step is even less satisfactory.[1−4] Classification of the excitation mechanisms into some limiting processes proposed by Durrup many years ago has been a useful guideline in the study of CID of polyatomic ions.[18] These are the pure electronic excitation via Franck−Condon transition ("process 1"), vibrational excitation via momentum transfer ("process 2"), vibronic excitation ("process 1−2"), and the excitation via the formation of a long-lived collision complex ("process 3"). According to recent investigations by Futrell and co-workers on the CID of simple polyatomic ions at superthermal energy,[19−23] substantial deflections of projectile ions accompany the energy transfer collisions, excluding the pure electronic excitation via Franck−Condon process as a viable mechanism. Also, the formation of a long-lived complex between the projectile and the target is not likely in the CID with noble gas targets at kiloelectronvolt translational energy. This leaves process 2 and 1−2 as the viable candidates for the energy transfer mechanism in the CID with noble gases at kiloelectronvolt energy. In process 2, momentum transfer to a part of the projectile results in its vibrational excitation, while electronic transition accompanying momentum transfer occurs in process 1−2 via mechanisms such as curve crossing. These processes are usually called vibrational excitation via momentum transfer and vibronic excitation via nonadiabatic interaction, respectively.[19,24] Another important finding is that, even though vibrational excitation via momentum transfer becomes more important at lower translational energy,[25−27] electronic (or vibronic) excitation is much more prevalent than was previously thought even at low translational energy.[19−23,28,29] For example, our recent investigation on the CID of methane molecular ion has shown that electronic excitation transferring 1−4 eV of internal energy[30] can compete with vibrational excitation transferring 0.2 eV at the center-of-mass collision energy of 200 eV.[28,29]

Another interesting development in this area in recent years is the observation of huge translational energy losses in the CID of large polyatomic ions such as polypeptide ions.[31−39] Large internal energy uptakes needed for the dissociation of systems with many degrees of freedom,[31] target excitation,[36] multiple collision,[39] etc., have been invoked to explain the huge energy losses. Even though many of these look plausible, a thorough experimental investigation is needed to find the cause(s) for such large energy losses. In particular, CID studies on heavy parent ions which do not consist of so many atoms as for

* To whom correspondence should be addressed.
[†] Present address: Analytical Technology Dept., LG Semicon Co., Ltd., 1 Hyangjeong-dong, Hungduk-gu, Cheongju-si 361-480, Korea
[⊗] Abstract published in *Advance ACS Abstracts,* August 1, 1997.

S1089-5639(96)04094-7 CCC: $14.00

polypeptide ions are needed to separate the mass effect from the degree of freedom effect.

Recently, we devised a method to obtain a scattering angular distribution from a mass-analyzed ion kinetic energy (MIKE) profile of a product ion generated by CID of a high mass ion.[24] This method has been applied to study the dynamics in CID of cesium iodide cluster ions, the following reactions in particular, the results from which being reported in this paper.

$$\underset{m/z\ 1691.8}{Cs_7I_6^+} \rightarrow \underset{m/z\ 1432.0}{Cs_6I_5^+} + CsI \quad (3)$$

$$\underset{m/z\ 1172.1}{Cs_5I_4^+} \rightarrow \underset{m/z\ 912.3}{Cs_4I_3^+} + CsI \quad (4)$$

Experimental Section

A double-focusing mass spectrometer with reversed geometry (VG Analytical, model ZAB-E) was used in this work. Cesium iodide cluster ions were generated by fast atom bombardment using an 8 keV xenon atom beam. Ions generated were accelerated to 2−9 keV translational energy. The parent ions were selected by the magnetic sector. The translational energy spectra of fragment ions generated by unimolecular dissociation of the parent ions, namely, metastable ion decomposition (MID),[40] or by CID occurring in the second field-free region of the instrument were obtained by scanning the voltages applied to the electric sector. This is the so-called mass-analyzed ion kinetic energy spectrometry (MIKES)[40] method. To induce CID, collision gas was introduced into the collision cell located near the intermediate focal point of the instrument. The collision cell was electrically floated at high voltage to reduce contributions from MID. The remaining MID signal was subtracted numerically. Collision gas pressure was adjusted to give 10−20 % attenuation of the parent ion beam. Peak distortion by multiple collisions was removed using the deconvolution technique developed recently.[41] The translational energy scale (abscissa) of a CID-MIKE profile was calibrated utilizing the peak position of the corresponding fragment ion in the MID-MIKE spectrum. H_2, D_2, He, Ne, Ar, and Xe were used as collision gases. The purities of the gases used were the highest commercially available and gas purifiers were used to remove water as much as possible.

Results and Discussion

Energetics in Collisions: An Overview. In MIKE spectrometry of a unimolecular reaction or metastable ion decomposition (MID), the average laboratory translational energy ($K_2°$) of the fragment ion m_2^+ of mass m_2 produced from the parent ion m_1^+ of mass m_1 with the translational energy of K_1 is well approximated by[40,42]

$$K_2° = (m_2/m_1)\, K_1 \quad (5)$$

Since a certain amount of the internal energy of m_1^+ or a distribution of energies is released as the relative translational energy of products, the laboratory translational energy K_2 of m_2^+ tends to show a distribution centered at $K_2°$.

When the same reaction occurs by CID, namely, via reactions 1 and 2, some of the initial laboratory translational energy of m_1^+ is lost elastically and inelastically in reaction 1. Even though the excitation of both m_1^+ and N (of mass N) can contribute to the inelastic energy loss Q, excitation of the latter has often been neglected when inert gases are used as targets because the energy gaps between the ground and the first excited electronic states of these are large. Conservation of energy in the laboratory coordinate system results in

$$K_1 = K_1' + K_N + Q \quad (6)$$

or

$$\Delta K_1 = K_1 - K_1' = K_N + Q \quad (7)$$

Here, K_1' and K_N are the postcollision translational energies of m_1^+ and N, respectively, and ΔK_1 is the translational energy loss of the parent ion. The center of the CID peak will be located at

$$K_2' = (m_2/m_1)K_1' \quad (8)$$

and the peak will be broadened due to the kinetic energy release. Distributions in K_N and Q further result in asymmetric tails usually on the lower translational energy side of the MIKE peak. Q cannot be larger than the translational energy for relative motion in the center-of-mass coordinate system K_{rel}.[4]

$$K_{rel} = \frac{N}{m_1 + N} K_1 \quad (9)$$

Even though Q in a collision event can have a range of value less than or equal to K_{rel}, Q in the CID generating a particular fragment ion, especially that produced by the least endoergic channels as considered in this work, would have a narrower distribution as dictated by the dissociation kinetics. Conservation of momentum leads to another important relation in the laboratory coordinate system.[4,43] Here, − and + represent the

$$\epsilon_N = (1+f)(2-q) - 2\cos^2\Theta \mp \sqrt{4\cos^2\Theta\,(\cos^2\Theta - (1+f)(1-f+fq))}/(1+f)^2 \quad (10)$$

forward ("soft") and backward ("hard") scattering, respectively.[4,44] Θ is the projectile deflection angle in the laboratory coordinate system, and ϵ_N, q, and f are defined as follows:

$$\epsilon_N = K_N/K_1 \quad (11)$$

$$q = Q/K_1 \quad (12)$$

$$f = N/m_1 \quad (13)$$

It is to be noted that K_N scales with K_1 when a CID process with well-defined Q is observed at a particular scattering angle. Also, K_N varies not only with K_1 but also with Θ under the MIKES conditions.

It is pertinent at this point to describe the energetics relationship derived by Uggerud and Derrick for vibrational−rotational excitation via a momentum transfer collision.[45] The theory, which was called impulsive collision theory (ICT) by the authors, is especially useful because some energetics and angular relations can be derived in analytic forms. In ICT, m_1^+ is divided into two parts, the impact and spectator portions. The elastic collision between the impact portion and the target is responsible for the energy loss of m_1^+ in the collision. Since the impact portion of the projectile may consist of one or more atoms, the collision may not be a binary one (atom−atom) in a strict sense. However, ICT will be regarded as a binary collision model in the rest of the paper because the impact portion is treated as an entity with a specific mass. The most important result in the ICT formalism is to find that ΔK_1 and Q, and hence K_N also, display the same angular dependences. Hence, the following relation between ΔK_1 and Q holds regardless of the scattering angle (N is the mass of N):

$$\Delta K_1 = (2\epsilon/\mu)Q \tag{14}$$

with

$$\epsilon = \frac{m_1\,(m_a + N)}{2N\,(m_1 - m_a)} \tag{15}$$

$$\mu = \left[1 - \frac{m_a N}{m_1\,(m_a + N)}\right]^{-1} \tag{16}$$

Here, m_a is the mass of the impact portion. Derrick and co-workers applied the ICT to various systems and claimed that it was more appropriate than the two-body collision model (as eqs 6−13).[34,35] It is to be emphasized, however, that the latter simply represents the conservations of energy and momentum and should hold regardless of the detailed collision model.

CID-MIKE Spectra. Since a conventional MIKE spectrometer has a small collection angle (several tenths of a degree), a fragment ion generated from a light parent ion highly deflected in a collision has little chance to be detected. As the parent ion mass increases, however, the laboratory scattering angle (Θ) corresponding to a given center-of-mass scattering angle (θ) decreases, allowing the detection of fragment ions generated from highly deflected parents. In elastic scattering, these two angles are related as follows:

$$\tan\Theta = \frac{\sin\theta}{\cos\theta + m_1/N} \tag{17}$$

For example, 90° scattering of $Cs_7I_6^+$ (m/z 1691.8) by He in the center-of-mass coordinate system corresponds to the laboratory scattering angle of 0.14°. The laboratory scattering angles become 0.68°, 1.4°, and 4.4° with Ne, Ar, and Xe collision gases, respectively. This means that fragment ions produced from highly deflected (in the center-of-mass coordinate system) parent ions can be detected in He CID while only those scattered in the forward direction contribute to the MIKE signal in Xe CID when the kinetic energy release is ignored.

The CID-MIKE spectra of $Cs_6I_5^+$ generated by reaction 3 with H_2, D_2, He, Ne, Ar, and Xe collision gases at 5 and 10 keV parent ion energies are shown in Figure 1. The similar data for reaction 4 are shown in Figure 2. The scale of abscissa (translational energy scale) in the figures is taken to be inversely proportional to $K_1^{1/2}$ in order to compare CID-MIKE profiles obtained at different translational energies. This is because the MIKE peak broadening arising from the kinetic energy release is proportional to $K_1^{1/2}$.[40,42] Its origin is taken at the corresponding MID-MIKE peak position.

Translational energy losses of the parent ions in the collision contributing to the spectra were calculated from the energy shift at the peak top. Namely,

$$\Delta K_1 = K_N + Q = (m_1/m_2)\,(K_2^\circ - K_2') \tag{18}$$

The results are summarized in Tables 1 and 2. It is seen that the energy loss estimated in this way decreases as the target mass increases (except H_2, to be explained). Of particular importance is the fact that the energy losses in CID with H_2, D_2, or He gases are even larger than K_{rel}. For example, ΔK_1 for reaction 3 with H_2 at 10 keV amounts to 28 eV while K_{rel} is only 12 eV. This means that K_N rather than Q is mainly responsible for the observed laboratory energy losses in CID with light targets.

As an attempt to investigate whether the energy loss could be explained by a binary collision, eqs 14−16 derived in the ICT model were used to evaluate Q from the energy loss. The

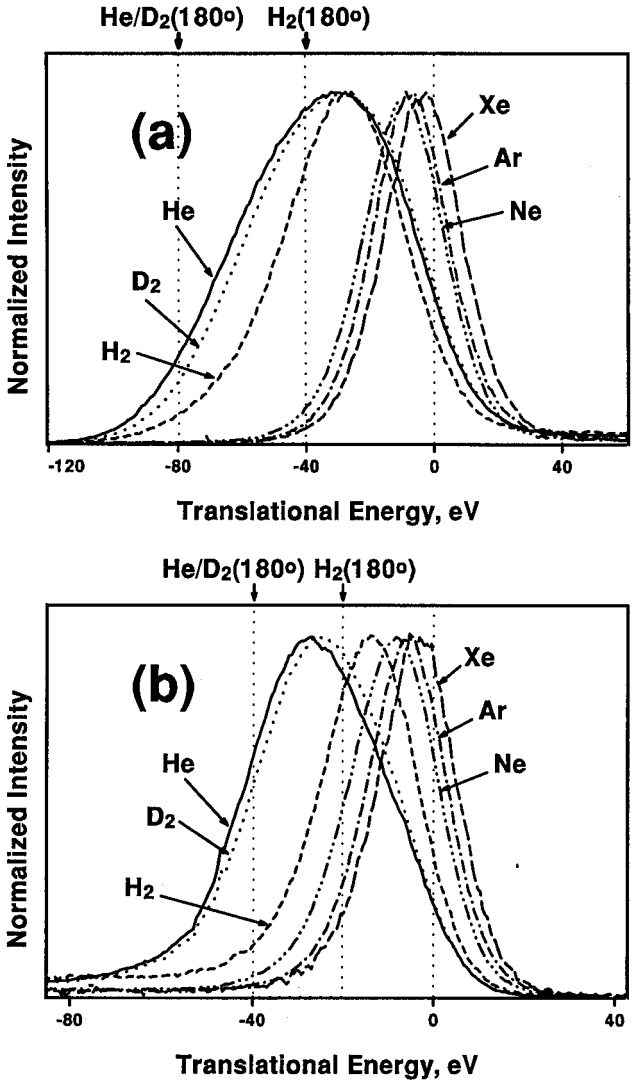

Figure 1. CID-MIKE profiles for reaction 3 at the parent ion translational energy of (a) 10 keV ($V = 9$ kV, $V' = -1$ kV) and (b) 5 keV ($V = 6$ kV, $V' = 1$ kV). V is the accelerating voltage in the ion source and V' is the voltage applied to the collision cell. Collision gases are H_2(− −), D_2(···), He(—), Ne(−···−), Ar(−·−), and Xe(− − −). The origin of the translational energy scale is taken at the corresponding MID-MIKE peak center. The energy scale is taken to be inversely proportional to $K_1^{1/2}$ (see text). Peak heights are normalized. The long tails with nearly constant intensity observed at higher (a) and lower (b) energy sides of CID-MIKE profiles are due to the dissociation between the cell and the grounded exit slit. The vertical dotted lines mark the laboratory translational energies of product ions generated from backscattered ($\theta = 180°$) parent ions in CID with He (or D_2) and H_2.

mass of the impact portion was taken as the average (129.9 u) of Cs and I masses. The results are listed in the parentheses in Tables 1 and 2. It is to be noted that Q thus estimated is only a fraction of ΔK_1, especially with the light targets, supporting the proposal that the large laboratory energy loss is mostly due to the elastic energy loss (K_N). Accepting the two step model for CID and the statistical picture (such as RRKM) for the dissociation step, one may expect that the inelastic energy transfer Q needed for a given channel, especially for the least endoergic ones, such as reactions 3 and 4 would be similar regardless of the laboratory translational energy and the target gas.[46] Data in Tables 1 and 2 show that this is the case with Ne, Ar, and Xe collision gases (to be called heavy gases). Diefenbach and Martin calculated the binding energies of the $Cs(CsI)_n^+$ cluster ions using the polarizable ion model.[47] The same model was used by Welch and co-workers to calculate

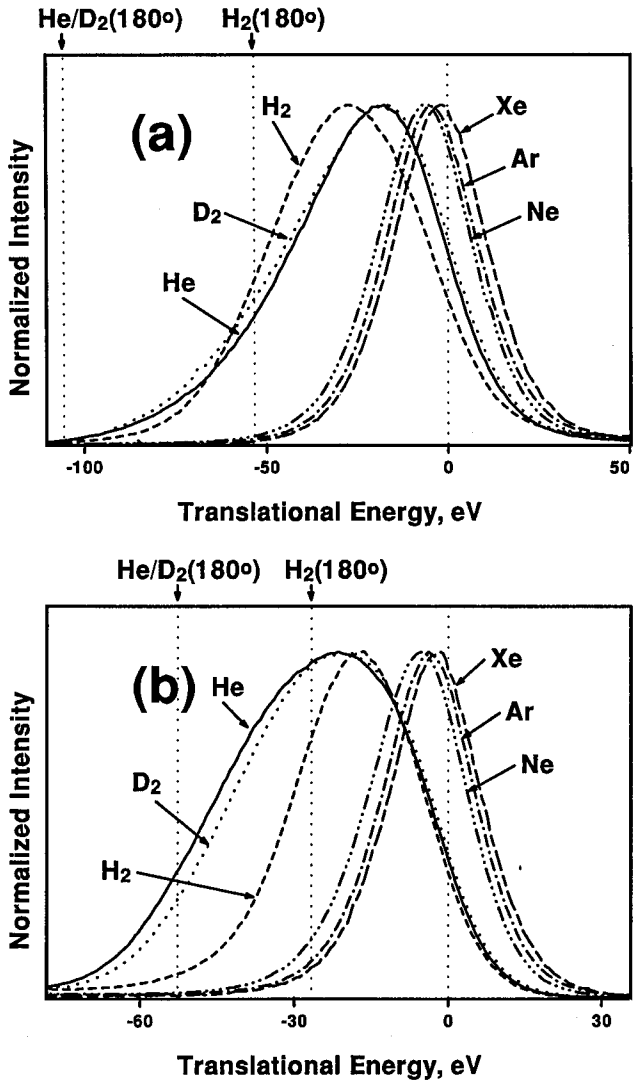

Figure 2. CID-MIKE profiles for reaction 4 at the parent ion translational energy of (a) 10 keV ($V = 9$ kV, $V' = -1$ kV) and (b) 5 keV ($V = 6$ kV, $V' = 1$ kV). See the caption of Figure 1.

the binding energy of CsI.[48] In this model, the potential terms due to the induced dipole moments arising from the fact that the electron shells are polarized by the electric field of other ions in a cluster are added to the rigid-ion potential. The thermochemical thresholds of the above reactions can be estimated by comparing the binding energies of the reactant and products. The thermochemical thresholds of ~1.7 and ~1.4 eV thus estimated for reactions 3 and 4, respectively, are also to ~1.5 and ~1.2 eV obtained from the present analysis. On the other hand, the estimated inelasticity varies with the laboratory translational energy and looks unphysical in CID with light collision gases (H_2, D_2, and He). Namely, the ICT model seems to be compatile with the energy losses observed with the heavy collision gases, but not with those with the light collision gases. According to the ICT model, vibrational excitation via momentum transfer becomes less efficient as the mass match between the impact portion and the target gets worse.[45] This suggests that the light collision gases would not be as efficient as the heavy ones in the present cases. The CID yields for reaction 3 obtained with He and Ne collision gases at the parent ion translational energy of 1−8 keV are shown in Figure 3. When the CID yields at the same K_{rel} are compared, He is found to be more efficient than Ne contrary to the above expectation. For example, the CID yield with He at 5 keV is larger by a factor of ~3 than that with Ne at 1 keV. This suggests that the energy transfer mechanisms in these two cases are different. If the energy transfer in CID with heavy collision gases occurs by vibrational excitation via momentum transfer, the same mechanism does not apply to CID with light collision gases.

Not only the average energy losses but also the overall peak patterns of the MIKE profiles in Figures 1 and 2 are of interest from a collision dynamics point of view. Two vertical dotted lines in each spectrum represent the laboratory translational energy of the product ions generated from the parent ions scattered elastically into the backward ($\theta = 180°$, $\Theta = 0°$) direction in a collision with H_2, D_2, or He. Namely, these correspond to the minimum laboratory energies for the product ions in each cases. Consideration of the inelastic energy transfer needed for dissociation would shift these lines slightly (~1 eV) toward the higher energy direction. (This is because the inelastic collision in the backward direction results in the postcollision projectile velocity vector located within the elastic scattering circle of the Newton diagram.) The fact that significant product ion intensities are observed in the left sides of these lines is due to the peak broadening arising from the kinetic energy release. In the case of heavy collision gases, the minimum laboratory energy lines are located far at the left sides of the MIKE profiles and are not drawn. As was explained earlier, the progressive downward shift of the MIKE profile with the decrease in the target mass except H_2 means higher elastic energy loss with lighter target. One may suppose that the higher instrumental discrimination with higher target mass at large scattering angle is mainly responsible for the above observation. This is not the case at least for the Ne CID because the detailed analysis of the MIKE profile carried out in the next section to determine the scattering angular distribution showed that the instrumental discrimination was not too significant. One of the most notable features in the figures is that the CID-MIKE profiles with D_2 and He are essentially identical, indicating the importance of the target mass in determining the elastic energy loss. The reason for the smaller energy loss with H_2 than with D_2 or He is also found in the target mass. Namely, the maximum elastic energy loss is less with H_2 than with D_2 or He as indicated by vertical dotted lines shown in the spectra. The physical meaning of the MIKE profile shift will become clearer when the scattering angular distributions are calculated from these profiles and compared.

Scattering Angular Distribution. The method to evaluate a scattering angular distribution from a CID-MIKE profile was described in detail previously.[24] The method to eliminate multiple collision effects was also reported.[41] Briefly, the CID-MIKE profile at a particular center-of-mass scattering angle, $C(K_2,\theta)$, is calculated analytically using the expression developed previously, which takes into account all the instrumental discriminations.[49] In the case of CID with Xe, the present instrument severely limits the observable center-of-mass scattering angle to the forward and backward regions as mentioned previously (eq 17). The translational energies of fragment ions generated in the backward scattering can be estimated by eq 10 which are much smaller than those observed. Namely, the observed CID-MIKE peak arises essentially from the forward scattering in the case of Xe. Using eq 10 again, it can be seen that the elastic energy transfer to Xe in the forward scattering is very small (2−3 eV) even in the worst cases. Namely, the large bandwidths of the CID-MIKE peaks are mainly due to the kinetic energy release in the dissociation step. Hence, the kinetic energy release distribution (KERD) in the reaction can be obtained by analyzing the CID-MIKE peak profile obtained with Xe. Then, the scattering angular distribution $P(\theta)$ is

TABLE 1: Average Translational Energy Losses of Parent Ions in the CID Reaction 3[a,b]

K_1	H_2	D_2	He	Ne	Ar	Xe
10 keV	24 ± 4	34 ± 2	34 ± 2	9.6 ± 1.0	6.5 ± 2.2	3.4 ± 1.3
	(0.24 ± 0.04)	(0.56 ± 0.04)	(1.1 ± 008)	(1.4 ± 0.1)	(1.7 ± 0.6)	(1.7 ± 0.6)
8 keV	24 ± 2	34 ± 2	39 ± 2	10 ± 1.0	6.7 ± 1.0	3.0 ± 0.8
	(0.20 ± 0.02)	(0.56 ± 0.02)	(1.3 ± 0.06)	(1.5 ± 0.2)	(1.7 ± 0.3)	(1.5 ± 0.4)
5 keV	15 ± 2	29 ± 2	31 ± 2	9.2 ± 1.0	6.3 ± 1.4	2.5 ± 0.8
	(0.13 ± 0.02)	(0.48 ± 0.02)	(1.0 ± 0.05)	(1.3 ± 0.1)	(1.6 ± 0.4)	(1.2 ± 0.4)
3 keV	11 ± 2	19 ± 2	19 ± 2	9.0 ± 1.0	6.1 ± 1.0	3.0 ± 0.8
	(0.09 ± 0.02)	(0.31 ± 0.02)	(0.60 ± 0.05)	(1.3 ± 0.1)	(1.6 ± 0.3)	(1.5 ± 0.4)
2 keV	7.8 ± 2	14 ± 2	13 ± 2	9.3 ± 2.0	5.7 ± 1.7	2.5 ± 0.8
	(0.06 ± 0.02)	(0.22 ± 0.02)	(0.42 ± 0.05)	(1.4 ± 0.3)	(1.5 ± 0.4)	(1.2 ± 0.4)
1 keV			7 ± 2	6.0 ± 1.5	6.0 ± 1.5	2.4 ± 1.2
			(0.23 ± 0.06)	(0.9 ± 0.2)	(1.6 ± 0.4)	(1.2 ± 0.6)

[a] Calculated from the translation energy of the CID-MIKE peak top using eq 18. Unit is in eV. [b] Inelastic energy losses (Q) calculated with the ICT formalism (eqs 14−16) are shown in parentheses. Unit is in eV.

TABLE 2: Average Translational Energy Losses of Parent Ions in the CID Reaction 4[a,b]

K_1	H_2	D_2	He	Ne	Ar	Xe
10 keV	32 ± 4	21 ± 2	22 ± 3	7.6 ± 1.2	5.4 ± 1.0	2.7 ± 1.0
	(0.28 ± 0.04)	(0.36 ± 0.03)	(0.75 ± 0.11)	(1.2 ± 0.2)	(1.5 ± 0.3)	(1.3 ± 0.5)
8 keV	29 ± 2	21 ± 2	23 ± 2	6.1 ± 1.0	4.9 ± 1.7	1.9 ± 1.0
	(0.25 ± 0.02)	(0.36 ± 0.03)	(0.77 ± 0.08)	(0.9 ± 0.2)	(1.3 ± 0.5)	(0.9 ± 0.5)
5 keV	21 ± 2	28 ± 7	25 ± 5	6.1 ± 1.0	5.4 ± 1.0	2.2 ± 1.3
	(0.18 ± 0.02)	(0.48 ± 0.12)	(0.85 ± 0.16)	(1.0 ± 0.2)	(1.5 ± 0.3)	(1.0 ± 0.6)
3 keV	14 ± 1	23 ± 2	23 ± 1	6.0 ± 1.0	4.0 ± 10	2.2 ± 1.0
	(0.12 ± 0.01)	(0.39 ± 0.03)	(0.77 ± 0.05)	(0.9 ± 0.2)	(1.0 ± 0.3)	(1.0 ± 0.5)
2 keV	9.8 ± 1	18 ± 2	18 ± 2	6.2 ± 1.0	3.7 ± 1.2	1.9 ± 1.3
	(0.08 ± 0.01)	(0.3 ± 0.03)	(0.61 ± 0.08)	(0.9 ± 0.2)	(1.0 ± 0.3)	(0.9 ± 0.6)

[a] Calculated from the translational energy of the CID-MIKE peak top using eq 18. Unit is in eV. [b] Inelastic energy losses (Q) calculated with the ICT formalism (eqs 14−16) are shown in parentheses. Unit is in eV.

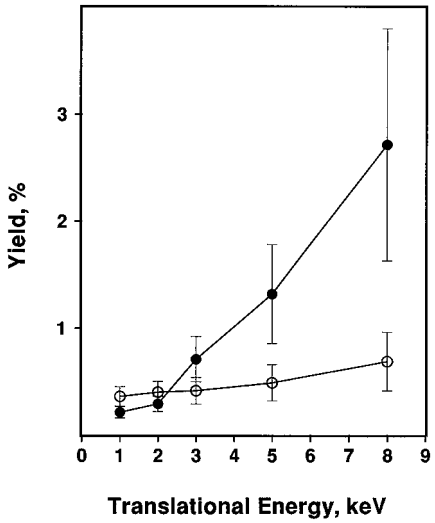

Figure 3. The CID yields for reaction 3 obtained with He (●) and Ne (○) collision gases at the parent ion translational energy of 1−8 keV. The parent ion beam was attenuated by 15%. The collision probability, instrumental discrimination, and detector sensitivity have been taken into account.[28]

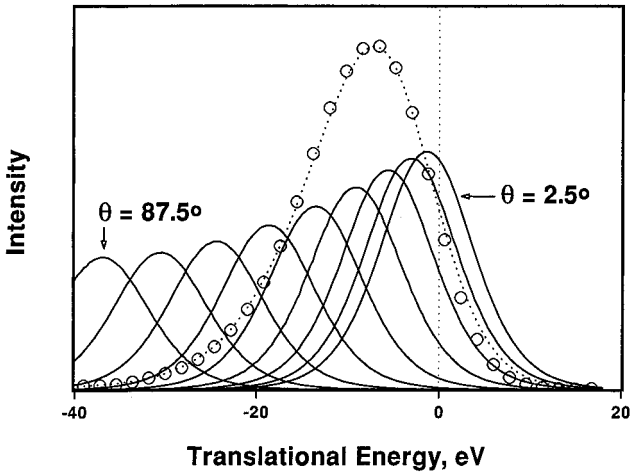

Figure 4. CID-MIKE profile for reaction 3 at 2 keV with Ne (○) and the C(K_2,θ) functions (—) at θ = 2.5°, 17.5°, 27.5°, 37.5°, 47.5°, 57.5°, 67.5°, 77.5°, and 87.5° (from right to left). The CID-MIKE profile recalculated from the fit is also shown (···). The origin of the translational energy scale is taken at the corresponding MID-MIKE peak center.

determined by fitting the experimental profile $F(K_2)$ with $C(K_2,\theta)$ functions:

$$F(K_2) = \sum P(\theta)\, C(K_2,\theta)\, \Delta\theta \qquad (19)$$

In the present cases, Q of 1.5 and 1.2 eV for reactions 3 and 4, respectively, were taken from the ICT analysis from heavy collision gases in Tables 1 and 2. Small variations in Q (0.5−2.5 eV) was found not to be important. KERDs have been determined from the Xe CID-MIKE profiles and C(K_2,θ) functions have been calculated for various cases. Some $C(K_2,\theta)$ functions evaluated for Ne CID of reaction 3 at the parent ion translational energy of 2 keV are shown in Figure 4. The best-fit profile determined with eq 19 is also compared with the experimental profile in the figure. It is to be emphasized that the instrumental discrimination has been fully accounted for in the calculation of $C(K_2,\theta)$ functions[49] and that a significant fraction of fragments generated by 90° scattering can be detected by the present instrument in the case of CID with Ne.

The scattering angular distributions for reactions 3 and 4 with H_2, D_2, He, and Ne collision gases are shown in Figures 5 and 6, respectively. The angular distributions in each figure are those determined at the same K_{rel}. For example, the distributions in Figure 5a are those for the H_2 CID at 10 keV, D_2 and HE CIDs at 5 keV, and Ne CID at 1 keV, all corresponding to K_{rel} of 12 eV. Similarly, K_{rel} values for those in Figures 5b and 6a,b are 23, 17, and 34 eV, respectively. It is remarkable to

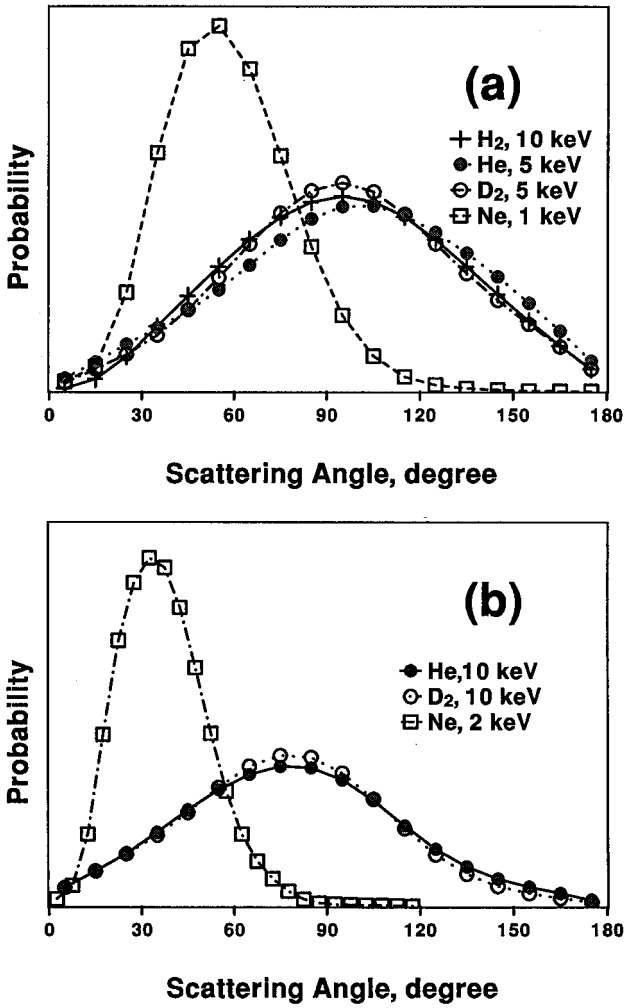

Figure 5. Normalized scattering angular distributions for reaction 3. (a) H_2 (+) at K_1 of 10 keV, He (●) and D_2 (○) at K_1 of 5 keV, and Ne (□) at K_1 of 1 keV. (b) He (●) and D_2 (○) at K_1 of 10 keV and Ne (□) at K_1 of K_1 of 2 keV.

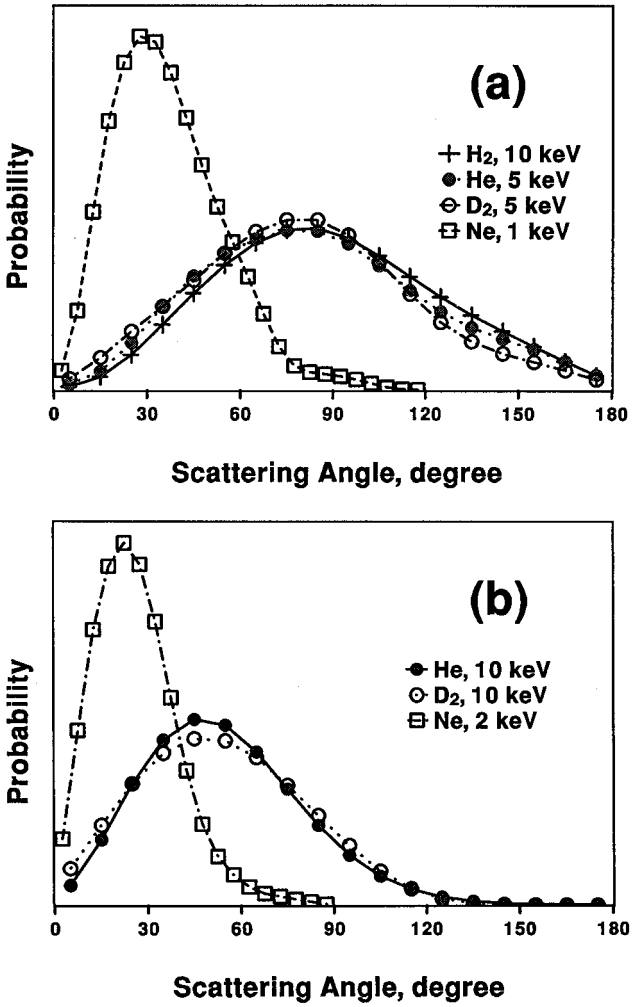

Figure 6. Normalized scattering angular distributions for reaction 4. (a) H_2 (+) at K_1 of 10 keV, He (●) and D_2 (○) at K_1 of 5 keV, and Ne (□) at K_1 of keV. (b) He (●) and D_2 (○) at K_1 of 10 keV and Ne (□) at K_1 of 2 keV.

note that the scattering angular distributions in CID with H_2, D_2, and He collision gases at the same K_{rel} are essentially the same both for reactions 3 and 4 while the angular distributions in Ne CID differ from these. This is an evidence supporting our previous observation of a dichotomy of the collision events into "light" and "heavy" target cases. Also, the fact that the distributions with H_2, D_2, and He are the same even though the masses of the constituting atoms vary from 1 to 4 can be taken as further evidence that vibrational excitation via binary collisions is not adequate to explain CID with light targets. Also noticed in Figures 5 and 6 is that the angular distribution moves toward larger angles as K_{rel} decreases. Namely, the energetics requirement favors a smaller impact parameter or larger scattering angle collision at lower K_{rel}, in agreement with the energetics consideration with the line-of-centers model.[50] In addition to reactions 3 and 4, CsI loss reactions by CID of $Cs_{14}I_{13}^+$, $Cs_{11}I_{10}^+$, $Cs_{10}I_9^+$, etc., have also been investigated. The MIKE profiles obtained for these reactions display the same tendency as for reactions 3 and 4.

If the reactions 3 and 4 in CID with heavy collision gases occur via vibrational excitation in a binary collision, their scattering angular distributions should be compatible with those predicted with the ICT formalism. In this regard, we have derived the expression for the scattering angular distribution of the parent ion dissociating via a specific channel. The details of the derivation are described in the Appendix. Briefly, the scattering angular distribution of the parent ion of a channel, $P_{ICT}(\theta)$, was expressed as a product of two angle-dependent terms:

$$P_{ICT}(\theta) \propto P_{ICT}^{\circ}(\theta)\, P_{diss}(\theta) \tag{20}$$

$P_{ICT}^{\circ}(\theta_s)$, which is the scattering angular distribution of the parent ion regardless of dissociation, was derived with the ICT formalism. $P_{diss}(\theta)$ embodies the dissociation energetics in the form

$$P_{diss}(\theta) \propto 2^{-(((Q(\theta)-Q^*)/\Delta)^2} \tag{21}$$

as assumed in the Appendix. Q^* and Δ characterize the center and width of the distribution. These are taken as the adjustable parameters related to the energetics window for a particular dissociation channel.

To calculate the scattering angular distributions for reaction 3, we have used the same values of Q^* and Δ regardless of K_1 and the target gas. These are 1.2 and 1.4 eV, respectively, which results in the average value of 1.5 eV for Q in agreement with the experimental result. The scattering angular distributions calculated for Ne CID at 1, 5, and 10 keV laboratory energies are compared with the experimental distributions in Figure 7. Considering various approximations adopted both in the experimental data analysis and in the theoretical development, the agreement between the experimental and calculated angular distributions is remarkable. In particular, the observation that

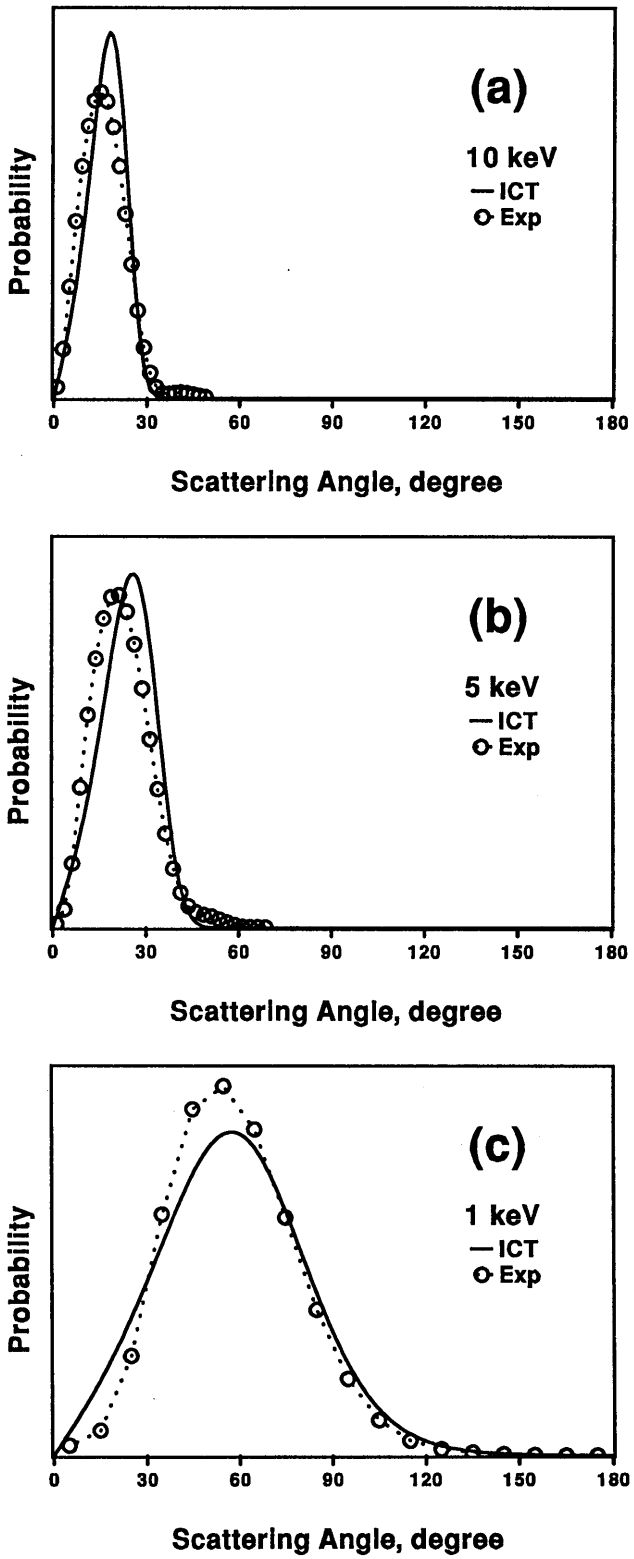

Figure 7. Experimental scattering angular distributions for reaction 3 with Ne (○) compared with the theoretical calculations based on ICT (—) at K_1 of (a) 10 keV, (b) 5 keV, and (c) 1 keV. Δ of 1.4 eV and Q^* of 1.2 eV were used for the calculations.

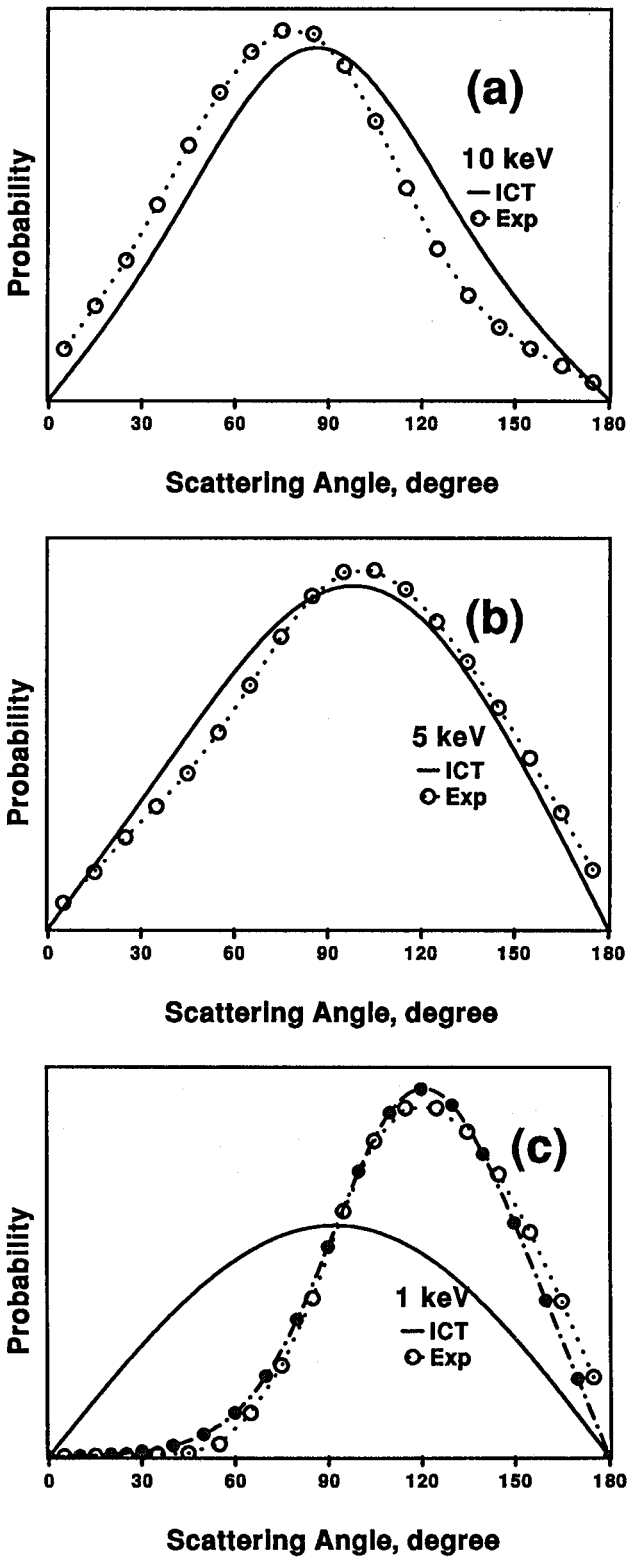

Figure 8. Experimental scattering angular distributions for reaction 3 with He (○) compared with the theoretical calculations based on ICT (—) at K_1 of (a) 10 keV, (b) 5 keV, and (c) 1 keV. Δ of 1.4 eV and Q^* of 1.2 eV were used for the calculations. Closed circles (●) in (c) are the calculated results with Q^* of 0.23 eV and Δ of 0.09 eV.

the scattering becomes more forward at the higher laboratory energy is well represented in the calculated distributions. It is to be mentioned, however, that the agreement between the experimental and calculated distributions is not a proof for the validity of the binary collision model because the calculated results depend sensitively on Q^* and Δ which are adjustable parameters. The most one can say is that the angular distribution in Ne CID can be explained within the binary collision model.

The same calculations have been performed for He CID. The results are shown in Figure 8. It is obvious that the agreement between the experimental and calculated results is not as good as for Ne CID. In particular, the calculated results are not as sensitive to the laboratory energy as the experimental ones.

The approach taken above to obtain the calculated angular distributions is simplistic in the sense that the internal energy

of the parent ion undergoing CID is not considered seriously. In fact, the experimental method used in this work generates the cluster ions with a wide range of internal energy. Most of the cluster ions with internal energy larger than the critical energy for the least endoergic reaction channel will dissociate by the time they arrive at the collision chamber. Hence, the internal energies of the CID parent ions will have a distribution up to the above critical energy, which is ~1.7 eV for the case of reaction 3 according to the previous estimation. At low K_{rel}, parent ions with low internal energy may not gain enough energy for dissociation in a collision. Namely, CID may occur only for the parent ions with the internal energy near the reaction threshold. In this regard, we attempted to fit the angular distribution for He CID of reaction 3 at 1 keV with smaller values of Q^* and Δ. Using 0.23 eV obtained in the ICT analysis of the peak shift in He CID at 1 keV as Q^*, a reasonably good fit was possible as shown in Figure 8c when Δ was taken as 0.09 eV. This means that only those parent ions with internal energy very near the threshold will dissociates in CID. Then, the CID yield with He will be much less than that with Ne at the same translational energy in which all the parent ions with the internal energy in the range 0−1.7 eV can be activated by collision into dissociation. In Figure 3, the CID yield at 1 keV with He is a little bit less than that with Ne. However, the difference does not seem to be large enough to support the momentum transfer excitation of the parent ions with internal energy near the threshold in the case of He CID. Also, if the momentum transfer excitation is responsible for CID with He and Ne, one would expect that the yield with Ne is larger than that with He because the former will result in a more energetic collision.[45] The fact that the CID yield with He is substantially larger than that with Ne at high parent ion translational energy in Figure 3 suggests that the excitation mechanism in He CID differs from that in Ne CID.

Excitation Mechanism. According to the analysis made so far on the magnitude of inelastic energy transfer, yield, and scattering angular distribution, vibrational excitation via momentum transfer seems to be compatible with CID of cesium iodide cluster ions with heavy collision gases. On the other hand, this mechanism of energy transfer does not look compatible with light target data especially at low collision energies. An alternative may be the excitation via formation of a long-lived collision complex ("process 3") mentioned in the introductory section. In fact, Fenselau and co-workers reported that formation of collision complexes can be an important excitation mechanism in CID of polypeptides ions with CH_4 and NH_3 collision gases.[51,52] Formation of a collision complex is not likely with noble gas targets for various reasons. For example, formation of a collision complex would result in an angular distribution which is more or less isotropic. Considering that this mechanism may be more important at smaller collision energy, one would expect more isotropic angular distribution at smaller energy contrary to the results in Figure 8. Hence, the only remaining alternative for CID with light targets is vibronic excitation via nonadiabatic interaction. Results from investigations made over the years on CID of polyatomic ions[1−4,18−29] also support the above conclusion. According to recent reports by Futrell and co-workers and also by us,[19−23,28,29] it is known that electronic (or vibronic) mechanism is prevalent even at lower K_{rel} than previously thought. Hence, occurrence of electronic excitation at Kr_{el} as low as 12 eV in the present study is not surprising in itself. It is surprising, however, to find that the energy transfer mechanism in CID with light targets is different from that with heavy targets. It is tempting to invoke the mass mismatch in light target cases and suggest that inefficiency of vibrational excitation with light targets makes vibronic mechanism look important.[45] This can be only partly true because the CID yield with He was found to be comparable to or larger than that with Ne. Without nonadiabatic calculations using models such as Landau−Zener curve crossing,[53−56] it is difficult to understand why electronic excitation is favored with light targets but not with heavy targets. Such calculations for systems as complicated as studied here look impractical at the moment. It is interesting to note that the light and heavy target dichotomy of the collisional excitation mechanism has been observed in CID of small and light parent ions also.[1−4,18]

Conclusion

Energetics and kinematics analyses of the MIKE profiles in CID of cesium iodide cluster ions have shown that the collision event can be classified into two groups: light and heavy target cases. In the heavy target case, the inelastic energy transfer calculated from the spectra using a binary collision model is nearly invariant with the laboratory translational energy and the target species (Ne, Ar, or Xe). The scattering angular distributions can be explained based on the binary collision model, suggesting the plausibility of vibrational excitation via momentum transfer in CID with heavy targets. This conclusion should be considered as tentative only, however, because the theoretical approach adopted to fit the experimental data contained some arbitrariness. The most remarkable finding in the light target case is that the scattering angular distribution is invariant with the target species (H_2, D_2, or He) as far as the center-of-mass translational energy is kept constant. This distribution could not be explained with the binary collision model, which suggests that the collisional excitation does not occur vibrationally but vibronically. At the moment, we do not understand why vibronic excitation is efficient in CID with light targets. Finally, it is to be emphasized that substantial laboratory energy losses have been observed in CID of cesium iodide cluster ions which are as heavy as but do not contain as many atoms as the polypeptide ions investigated previously when light targets are used. In our evaluation of the scattering angular distribution from a CID-MIKE spectrum, target gases are differentiated only in their masses. Then, the fact that the scattering angular distributions obtained with H_2, D_2, and He are virtually identical even though the energy loss with H_2 is different from those with D_2 and He looks particularly indicative. Namely, the large energy losses observed with light targets in CID of cesium iodide cluster ions must originate from the elastic energy transfer to the target as assumed in the present analysis. In this regard, it is worthwhile to extend the present approach to CID of heavy ions consisting of many atoms to see if a similar explanation is applicable to the substantial energy losses observed in those systems.

Appendix

Scattering Angular Distribution in CID Occurring via Binary Collision. In this Appendix, we will attempt to derive the scattering angular distribution of the parent ion in CID to a particular fragment ion using the ICT formalism developed by Uggerud and Derrick.[45] Some of the initial part of the derivation reported by these authors will be repeated for ease of presentation. The key assumption in ICT is that energy and momentum transfers take place by an elastic hard sphere collision between the target and the impact portion of the projectile. Another assumption made to simplify the mathematical treatment is that the projectile is deflected only in the y direction of the instrument used. (x is the direction of the principal ion−optical axis of the instrument, or the direction of the projectile

movement. *y* is the direction of the electric field of the electric sector of a double-focusing mass spectrometer.)[49] The velocities of the projectile and the target $\vec{\omega}_1$ and $\vec{\omega}_N$ in the center-of-mass coordinate system are expressed as follows.

$$\vec{\omega}_1 = \frac{N}{m_1 + N}\vec{v} \tag{A.1}$$

$$\vec{\omega}_N = -\frac{m_1}{m_1 + N}\vec{v} \tag{A.2}$$

Here, $\vec{v}$ represents the velocity of the projectile in the laboratory coordinate system. Conservation of momentum in the *x* and *y* directions applied to the collision between the impact portion and the target with masses m_a and *N* gives

$$m_a\omega_1 + N\omega_N = m_a\omega_{ax}' + N\omega_{Nx}' \tag{A.3}$$

$$0 = m_a\omega_{ay}' + N\omega_{Ny}' \tag{A.4}$$

Conservation of energy gives

$$1/2m_a\omega_1^2 + 1/2N\omega_N^2 = 1/2m_a\omega_{ax}'^2 + 1/2N\omega_{Nx}'^2 + 1/2m_a\omega_{ay}'^2 + 1/2N\omega_{Ny}'^2 \tag{A.5}$$

Taking the impact portion and the target as hard spheres, the impact angle ϕ is defined as the angle between the *x*-axis and the line-of-centers of two colliding particles. Namely,

$$\sin\phi = b/d \tag{A.6}$$

Here, *b* and *d* represent the impact parameter and the hard sphere distance between two colliding particles. Conservation of angular momentum results in

$$\omega_{Ny}' = -(\omega_{Nx}' - \omega_{Nx})\tan\phi \tag{A.7}$$

Solving eqs A.3−A.7, postcollision velocity components of the impact portion of the projectile and the target are obtained:

$$\omega_{ax}' = \frac{N}{m_1 + N}v - \frac{2\,N\cos^2\phi}{m_a + N}v \tag{A.8a}$$

$$\omega_{Nx}' = -\frac{m_1}{m_1 + N}v + \frac{2m_a\cos^2\phi}{m_a + N}v \tag{A.8b}$$

$$\omega_{ay}' = \frac{2N\sin\phi\cos\phi}{m_a + N}v \tag{A.8c}$$

$$\omega_{Ny}' = -\frac{2\,m_a\sin\phi\cos\phi}{m_a + N}v \tag{A.8d}$$

Equations (A.8a−A.8d) are the same as those reported by Uggerud and Derrick, except for some changes in notation. Now we will proceed to derive the expression for the scattering angular distribution in the center-of-mass coordinate system. The change in the momentum of m_a induced by the collision eventually leads to the change in the momentum of the whole projectile. Considering that the momentum of the whole projectile is conserved after the collision, the following expressions are obtained for the velocity components in the center-of-mass coordinate system of the whole projectile:

$$\omega_x' = \frac{(m_1 - m_a)\omega_1 + m_a\omega_{ax}'}{m_1} = \frac{N}{m_1 + N}v - \frac{2\,m_a N\cos^2\phi}{m_1(m_a + N)}v \tag{A.9}$$

$$\omega_y' = \frac{m_a}{m_1}\omega_{ay}' = \frac{2m_aN\sin\phi\cos\phi}{m_1(m_a + N)}v \tag{A.10}$$

Conservation of energy during the postcollision period is as follows:

$$1/2(m_1 - m_a)\omega_1^2 + 1/2m_a\omega_{ax}'^2 + 1/2m_a\omega_{ay}'^2 = 1/2m_1\omega_x'^2 + 1/2m_1\omega_y'^2 + Q \tag{A.11}$$

Substituting eqs A.1 and A.8−A.10 into eq A.11, the expression for *Q* is obtained:

$$Q = 4\frac{m_aN^2(m_1 - m_a)}{m_1^2(m_a + N)^2}K_1\cos^2\phi \tag{A.12}$$

This expression is the same as the one reported by Uggerud and Derrick which was derived with the laboratory coordinate system. The center-of-mass scattering angle θ is related to ϕ as follows:

$$\tan\theta = \frac{\omega_y'}{\omega_x'} = \frac{\sin\phi\cos\phi}{m_1(m_a + N)/2m_a(m_1 + N) - \cos^2\phi} \tag{A.13}$$

This can be rearranged as follows:

$$\sin(2\phi + \theta) = g\sin\theta \tag{A.14}$$

with

$$g = \frac{N(m_1 - m_a)}{m_a(m_1 + N)} \tag{A.15}$$

Considering that θ and ϕ span 0°−180° and 0°−90°, respectively, the following relation is obtained:

$$\phi = 1/2(\pi - \theta - \sin^{-1}(g\sin\theta)) \tag{A.16}$$

Then, the scattering angular distribution in the binary collision (ICT) is derived as follows:

$$P_{ICT}°(\theta) = 2\pi b\left|\frac{db}{d\theta}\right| = 2\pi b\left|\frac{db}{d\phi}\right|\left|\frac{d\phi}{d\theta}\right| = 1/2\pi d^2\sin[\sin^{-1}(g\sin\theta) + \theta] \times \left(1 + \frac{g\cos\theta}{\sqrt{1 - g^2\sin^2\theta}}\right) \tag{A.17}$$

It is important to note that eq A.17 is the scattering angular distribution of the projectile in a binary collision. In general, this would be different from the scattering angular distribution of the parent ion dissociating via a particular channel, because the energetics of the channel is involved in the latter. In this regard, it is to be noted that *Q* is also a function of the scattering angle (eq A.12) and that a given channel usually occurs within a rather well defined internal energy range. Namely, the least endoergic channel will be favored at small scattering angle while the dissociation will be dominated by more endoergic ones at large angle according to ICT. To take into account the dissociation energetics, the scattering angular distribution in CID, $P_{ICT}(\theta)$, will be expressed here as a product of $P_{ICT}°(\theta)$

and the angle-dependent dissociation probability $P_{diss}(\theta)$.

$$P_{ICT}(\theta) \propto P_{ICT}^{\circ}(\theta)P_{diss}(\theta) \quad \text{(A.18)}$$

We will further assume that $P_{diss}(\theta)$ is a Gaussian type function centered at Q^* with the half width Δ. Namely,

$$P_{diss}(\theta) \propto 2^{-((Q(\theta)-Q^*)/\Delta)^2} \quad \text{(A.19)}$$

$Q(\theta)$ is readily derived from eqs A.12 and A.16:

$$Q = 2\frac{m_a N^2(m_1 - m_a)}{m_1^2(m_a + N)^2}K_1[1 - \cos\{\sin^{-1}(g \sin\theta) + \theta\}] \quad \text{(A.20)}$$

Namely, we can calculate the scattering angular distribution in CID occurring via binary collision by choosing appropriate values of Δ and Q^*.

Acknowledgment. This work was financially supported by Ministry of Education, Republic of Korea, and by the Korea Science and Engineering Foundation (KOSEF) through the Center for Molecular Catalysis at Seoul National University. Y.J.L. gratefully acknowledges the support of a Daewoo Foundation Post-Graduate Scholarship, 1995.

References and Notes

(1) Cooks, R. G. In *Collision Spectroscopy*; Cooks, R. G., Ed.; Plenum: New York, 1978; Chapter 7.
(2) Bordas-Nagy, J.; Jennings, K. R. *Int. J. Mass Spectrom. Ion Processes* **1990**, *100*, 105.
(3) McLuckey, S. A. *J. Am. Soc. Mass Spectrom.* **1992**, *3*, 599.
(4) Kim, M. S. *Org. Mass Spectrom.* **1991**, *26*, 565.
(5) Jennings, K. R. *Int. J. Mass Spectrom. Ion Phys.* **1968**, *1*, 227.
(6) McLafferty, F. W.; Bente, P. F., III; Kornfeld, R.; Tsai, S.-C.; Howe, I. J. *J. Am. Chem. Soc.* **1973**, *95*, 2120.
(7) McLafferty, F. W., Ed. *Tandem Mass Spectrometry*; Wiley: New York, 1983.
(8) Busch, K. L.; Glish, G. L.; McLuckey, S. A. *Mass Spectrometry/Mass Spectrometry*; VCH: New York, 1988.
(9) Los, J.; Govers, T. R. In *Collision Spectroscopy*; Cooks, R. G., Ed.; Plenum: New York, 1978; Chapter 6.
(10) Green, T. A.; Peek, J. M. *Phys. Rev.* **1969**, *183*, 166.
(11) Green, T. A. *Phys. Rev. A* **1970**, *1*, 1416.
(12) Lee, Y. J.; Kim, M. S. *Chem. Phys. Lett.* **1992**, *192*, 89. Lee, Y. J.; Kim, M. S. *J. Phys. Chem.* **1993**, *97*, 1119; Lee, Y. J. Kim, M. S. *Rapid Commun. Mass Spectrom.* **1993**, *7*, 994.
(13) Forst, W. *Theory of Unimolecular Reactions*; Academic: New York, 1973.
(14) Rosenstock, H. M.; Wallenstein, M. B.; Wahrhaftig, A. L.; Eyring, H. *Proc. Natl. Acad. Sci. U.S.A.* **1952**, *38*, 667.
(15) Schlag, E. W.; Levine, R. D. *Chem. Phys. Lett.* **1989**, *163*, 523.
(16) Bernshtein, V.; Oref, I. *J. Phys. Chem.* **1994**, *98*, 136.
(17) Rockwood, A. L.; Busman, M.; Smith, R. D. *Int. J. Mass Spectrom. Ion Processes* **1991**, *111*, 103.
(18) Durup, J. In *Recent Developments in Mass Spectrometry*; Ogata, K., Hayakawa, T., Eds.; University Park Press: Baltimore, 1969; p 21.
(19) Shukla, A. K.; Futrell, J. H. *Mass Spectrom. Rev.* **1993**, *12*, 211.
(20) Qian, K.; Shukla, A. K.; Howard, S. K.; Anderson, S. G.; Futrell, J. H. *J. Phys. Chem.* **1989**, *93*, 3889.
(21) Qian, K.; Shukla, A. K.; Futrell, J. H. *J. Chem. Phys.* **1990**, *92*, 5988.
(22) Shukla, A. K.; Qian, K.; Anderson, S. G.; Futrell, J. H. *Int. J. Mass Spectrom. Ion Processes* **1991**, *109*, 227.
(23) Qian, K.; Shukla, A. K.; Futrell, J. H. *J. Am. Chem. Soc.* **1991**, *113*, 7121.
(24) Lee, Y. J.; Kim, M. S. *J. Chem. Phys.* **1995**, *103*, 5442.
(25) McLuckey, S. A.; Ouwerkerk, C. E. D.; Boerboom, A. J. H.; Kistemaker, P. G. *Int. J. Mass Spectrom. Ion Processes* **1984**, *59*, 85.
(26) Yamaoka, H.; Pham, D.; Durup, J. *J. Chem. Phys.* **1969**, *51*, 3465.
(27) Refaey, K. M.; Chupka, W. A. *J. Chem. Phys.* **1965**, *43*, 2544.
(28) Kim, B. J.; Kim, M. S. *Rapid Commun. Mass Spectrom.* **1990**, *4*, 327.
(29) Lee, H. S.; Kim, M. S. *J. Phys. Chem.* **1996**, *100*, 1459.
(30) Berkowitz, J.; Greene, J. P.; Cho, W. H.; Ruscic, B. *J. Chem. Phys.* **1987**, *86*, 674.
(31) Neumann, G. M.; Derrick, P. J. *Org. Mass Spectrom.* **1984**, *19*, 165.
(32) Sheil, M. M.; Derrick, P. J. *Org. Mass Spectrom.* **1988**, *23*, 429.
(33) Neumann, G. M.; Sheil, M. M.; Derrick, P. J. *Z. Naturforsch.* **1984**, *A39*, 584.
(34) Derrick, P. J.; Colburn, A. W.; Sheil, M. M.; Uggerud, E. *J. Chem. Soc., Faraday Trans.* **1990**, *86*, 2533.
(35) Bradley, C. D.; Curtis, J. M.; Derrick, P. J.; Sheil, M. M. *J. Chem. Soc., Faraday Trans.* **1994**, *90*, 239.
(36) Bricker, D. L.; Russell, D. H. *J. Am. Chem. Soc.* **1986**, *108*, 6174.
(37) Alexander, A. J.; Thibault, P.; Boyd, R. K. *J. Am. Chem. Soc.* **1990**, *112*, 2484.
(38) Thibault, P.; Alexander, A. J.; Boyd, R. K. *J. Am. Soc. Mass Spectrom.* **1993**, *4*, 835.
(39) Bradley, C. D.; Derrick, P. J. *Org. Mass Spectrom.* **1991**, *26*, 395.
(40) Cooks, R. G.; Beynon, J. H.; Caprioli, R. M.; Lester, G. R. *Metastable Ions*; Elsevier: Amsterdam, 1973.
(41) Lee, Y. J.; Kim, M. S. *Int. J. Mass Spectrom. Ion Processes*, in print.
(42) Yeh, I. C.; Kim, M. S. *Rapid Commun. Mass Spectrom.* **1992**, *6*, 115.
(43) Appel, J. In *Collision Spectroscopy*; Cooks, R. G., Ed.; Plenum: New York, 1978; Chapter 4.
(44) Boyd, R. K.; Kingston, E. E.; Brenton, A. G.; Beynon, J. H., *Proc. R. Soc. London* **1984**, *A392*, 59.
(45) Uggerud, E.; Derrick, P. J. *J. Phys. Chem.* **1991**, *95*, 1430. Cooper, H. J.; Derrick, P. J.; Jenkins, H. D. B.; Uggerud, E. *J. Phys. Chem.* **1993**, *97*, 5443.
(46) Cooks, R. G.; Hendricks, L.; Beynon, J. H. *Org. Mass Spectrom.* **1975**, *10*, 625.
(47) Diefenbach, J.; Martin, T. P. *J. Chem. Phys.* **1985**, *83*, 4585.
(48) Welch, D. O.; Lazareth, O. W.; Dienes, G. J.; Hatcher, R. D. *J. Chem. Phys.* **1978**, *68*, 2159.
(49) Lee, Y. J.; So, H. Y.; Kim, M. S. *Rapid Commun. Mass Spectrom.* **1994**, *8*, 571.
(50) Smith, I. W. M. *Kinetics and Dynamics of Elementary Gas Reactions*; Butterworth: London, 1980.
(51) Orlando, R.; Fenselau, C.; Cotter, R. J. *J. Am. Soc. Mass Spectrom.* **1991**, *2*, 189.
(52) Cheng, X.; Fenselau, C. *J. Am. Chem. Soc.* **1993**, *115*, 10327.
(53) Bernstein, R. B. *Atom-Molecule Collision Theory*; Plenum: New York, 1979.
(54) Nakamura, H. *Int. Rev. Phys. Chem.* **1991**, *10*, 123.
(55) Nikitin, E. E.; Umanskii, S. Ya. *Theory of Slow Atomic Collisions*; Springer: Berlin, 1984.
(56) Zhu, C.; Nakamura, H. *J. Chem. Phys.* **1995**, *102*, 7448.